World Scientific
www.worldscientific.com

AUTOMATED EXTRACTION OF THE INNER CONTOUR OF THE ANTERIOR CHAMBER USING OPTICAL COHERENCE TOMOGRAPHY IMAGES

PENG SHU* and YANKUI SUN†

Department of Computer Science and Technology
Tsinghua University, Beijing 100084, P. R. China
*shupemg@gmail.com
†syk@mail.tsinghua.edu.cn

Manual analysis of anterior segment optical coherence tomography (AS-OCT) images is fairly time consuming, and inter-observer reproducibility cannot be guaranteed. Therefore, auto-mated analysis methods of AS-OCT images are necessary in clinical applications. This paper presents a novel approach to extract the inner contour of the anterior chamber automatically from AS-OCT images using a "divide-and-conquer" strategy. We first find the anchor points in an image and these points are used to divide the image into subimages where the iris, lens and cornea are located. Then the endothelial surface of the cornea, lens surface and iris surface are obtained from these subimages with different schemes, and they are merged together to obtain the complete inner contour. In our method, the endothelial surface of the cornea is fitted by using three circular arcs under continuity constraints. Experiments show that the proposed algorithm can extract the inner contour of the anterior chamber from AS-OCT images accu-rately in real time.

Keywords: Computer-aided diagnosis; endothelial surface of the cornea; divide-and-conquer strategy.

1. Introduction

Optical coherence tomography (OCT)[1] is an ima-ging method that allows high-resolution cross-sec-tional images to be obtained through tissues and materials, similar to an ultrasound image. With the use of anterior segment optical coherence tom-ography (AS-OCT), we are able to obtain high-resolution, cross-sectional images of the anterior chamber, which enables the assessment of many quantitative parameters such as the central cornea thickness, pupil diameter, anterior chamber volume (ACV) and depth. Knowledge of ACV is useful in ocular pharmacokinetics, aqueous humor dynamics and primary angle-closure and pigmentary glau-coma.[2] Anterior chamber depth is useful for the evaluation of a number of conditions affecting the

---

†Corresponding author.

eye, including angle-closure glaucoma, and also for postoperative follow-up of cataract surgery with phakic intraocular lens implantation.[3] Central cornea thickness and pupil diameter are useful too. As is well known, manual analysis of AS-OCT images is fairly time consuming, and inter-observer reproducibility cannot be guaranteed. If we can extract the inner contour of the anterior segment chamber automatically, then the related quantitative parameters can be obtained easily. Unfortunately, AS-OCT images are often affected by speckle noise and light beam crossings. Different parts of an image can vary in pixel distribution, and edge delineation of some parts may be strong while others are often weak and discontinuous. Some work has been done to segment parts of the anterior chamber. Graglia extracted the corneal contour from AS-OCT radial images automatically using a contour detection algorithm that works pixel-by-pixel.[4] Coron developed an algorithm to segment the anterior chamber of eye ultrasound images automatically using a single circle to fit surfaces of the cornea. They assumed that the epithelial surface shared the same circle center with the endothelial surface.[5] Lin expanded the algorithm of Coron to AS-OCT image processing using an iterative algorithm to remove the effect of light beam cross lines, and they assumed that the upper and lower boundary of the cornea shared the same circle center with the boundary of the lens,[6] which is not reasonable for most of our images. The software embedded in Visante OCT or Slit-Lamp OCT has the ability to segment AS-OCT images, but to our knowledge, their algorithms have not been published.[7] In this paper, we describe the design of an automated algorithm to analyze AS-OCT images and extract the inner contour of the anterior chamber. The divide-and-conquer strategy is proposed to process different parts of the AS-OCT images with different schemes, where the endothelium surface of cornea is fitted by using three circular arcs under continuity constraints. Experiments on many images show that our algorithm can extract the inner contour of anterior chamber from AS-OCT images accurately in real time.

This paper is organized as follows: Sec. 2 provides a brief description of random sample consensus (RANSAC) algorithm, which is used in our method. Section 3 discusses the proposed method in detail. Experimental results are given in Sec. 4. Discussions are done in Sec. 5. Conclusions are made in Sec. 6.
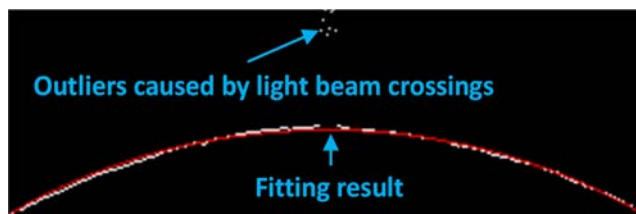

Fig. 1. Fit circles with RANSAC algorithm. The white points are the epithelial surface of the central cornea detected by canny edge detector,[9] which contains some outliers caused by light beam crossings. The red circular arc is the fitted result by RANSAC algorithm.

2. RANSAC Algorithm

RANSAC is an abbreviation for "random sample consensus". It is an iterative method for fitting a model from a set of observed data which contains a significant percentage of gross errors.[8]

In this paper, the RANSAC algorithm is used to fit circles, which works as follows:

(1) Draw a sample from the data uniformly and randomly.
(2) Fit a circle to the sample, using the least squares method.
(3) For each point outside the sample, the distance from the point to the circle is computed; if the distance is small enough, we call the point is close to the circle.
(4) If the number of points close to the circle is great enough, then this is a good fit, and the circle is refitted using the sample and all the close points.
(5) Iterate Steps (1)–(4) for some time, and then select the best fit using the fitting error as a criterion.

An example is shown in Fig. 1.

3. Proposed Method

The anterior chamber is composed of tissues that present different characteristics in AS-OCT images. The signal of the iris is very strong with a clear edge, while the signal of the peripheral cornea is a little weak with an edge that is often discontinuous. Also, the images are usually affected by speckle noise. Therefore, it is difficult to extract an accurate inner contour from AS-OCT images by using classic global image segmentation algorithms directly. Here we propose a "divide-and-conquer" method to resolve this problem. Some anchor points with obvious features are first found, and they are used
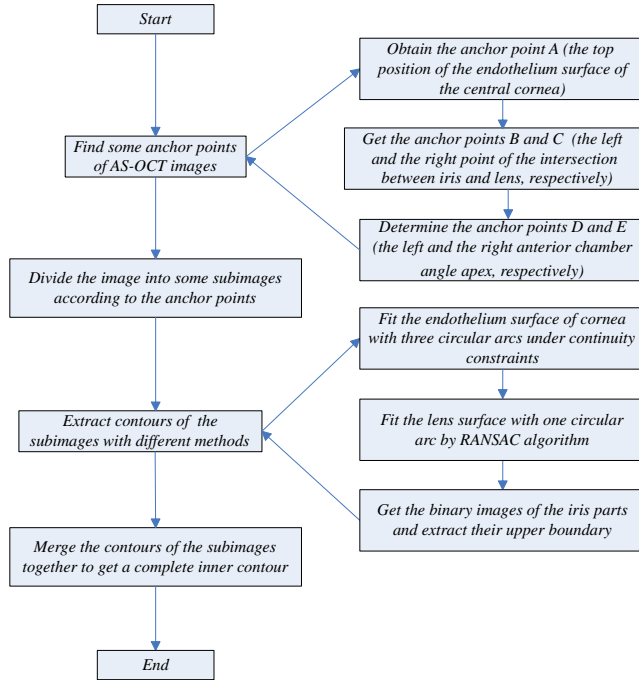
Fig. 2.   Flowchart of our method.

to divide the AS-OCT image into subimages, where the iris, lens and cornea located in different subimages. Then, the contour of the subimages are extracted with different schemes, and they are merged together to obtain the complete inner contour. Figure 2 illustrates the flowchart of our method.

3.1. *Finding the anchor points in AS-OCT images*

The anchor points A, B, C, D and E that are to be found are shown in Fig. 3(a). We describe these anchor points as:

3.1.1. *Anchor point A*

The epithelial surface of the central cornea is clear in almost all AS-OCT images and, therefore, it can be detected very easily. It is then fitted with a single circle, where the RANSAC[8] algorithm is employed so as to remove the effect of light beam crossings, as is shown in Fig. 1. Since the endothelial surface is beneath the epithelial surface, and the distance between them is defined as the central cornea thickness, we can estimate it first. Then the endothelial surface of the central cornea is detected based on the epithelial surface, and it is further

fitted by another circle with RANSAC algorithm. Finally, the top position of the endothelial surface of the central cornea is found and denoted as the anchor point A.

3.1.2. *Anchor points B and C*

Since the lens surface is beneath the endothelial surface of the central cornea, we can get a subimage I_1 [Fig. 3(b)] from the AS-OCT image that contains the whole lens and part of the iris, where the signal intensity of the iris is much stronger than that of the lens. By summing the pixel values of each column of I_1, we get a curve C_1 [Fig. 3(c)], whose two points of discontinuity can be detected as the horizontal coordinates of anchor points B and C. The point of discontinuity of the A-scan with the same horizontal coordinates as B/C in I_1 can be detected easily, which marks the vertical coordinates of the anchor point B/C.

3.1.3. *Anchor points D and E*

In our experimental data, the signal in the nearby region of the anterior chamber angle apex is very strong. When heavy dilation and erosion are operating, filters such as the median filter, Gaussian filter and threshold filter are applied to the AS-OCT image, so a binary image I_2, as is shown in Fig. 3(d), is obtained, where the left anterior chamber angle apex is very clear and can be detected as the preliminary estimate of the anchor point D. The estimated position of the anchor point D is a little away from the real position because of the dilation and erosion operation. To get its accurate position, we extract a small region from the original image around the point D, denoted as I_3 in Fig. 3(a). The median filter, Gaussian filter and threshold filter are applied to I_3, and the small connected regions are detected and filled in, so a binary image I_3' of I_3, consisting of two connected regions, is obtained and the left apex point of the largest dark region is considered as the anchor point D. The anchor point E can be determined similarly.

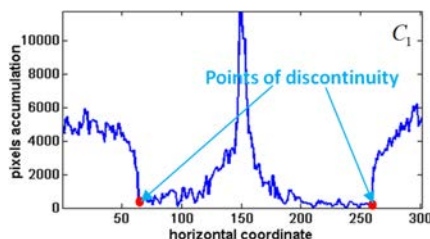### 3.2. *Dividing the image into subimages*

By using the anchor points obtained above, we split the image into six parts, which are separated by yellow lines in Fig. 3(a). The iris is located in Areas I and II, the cornea in the Area III and the lens in the
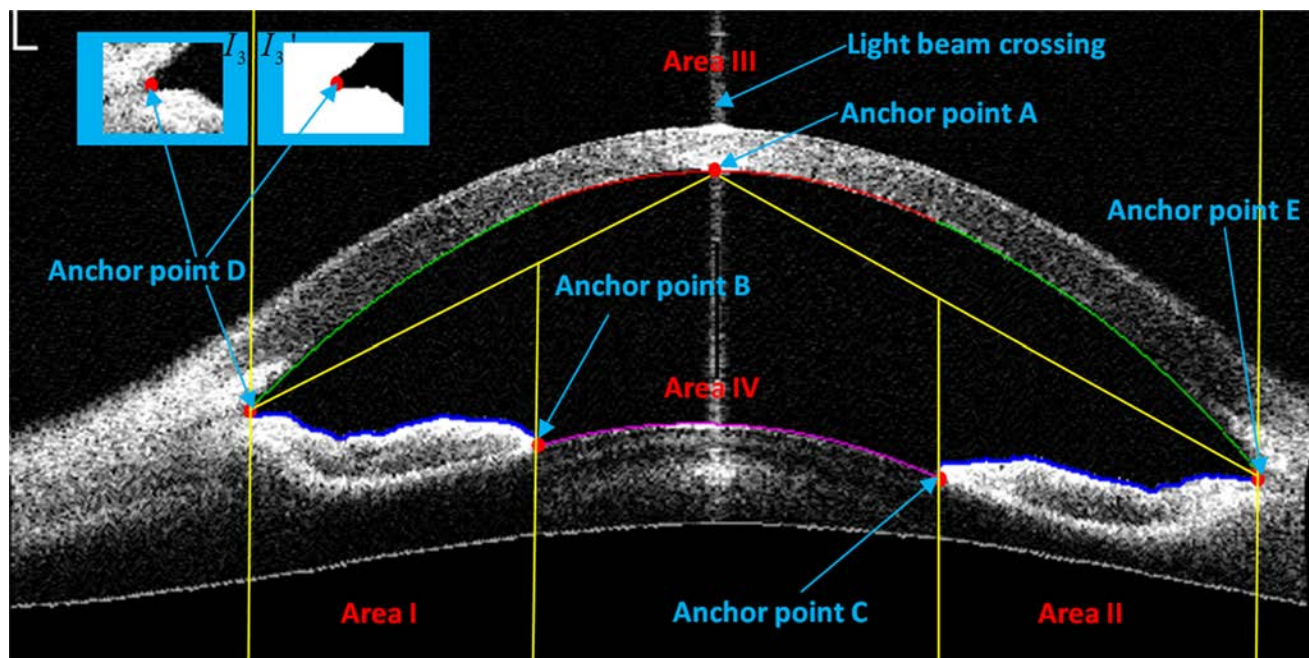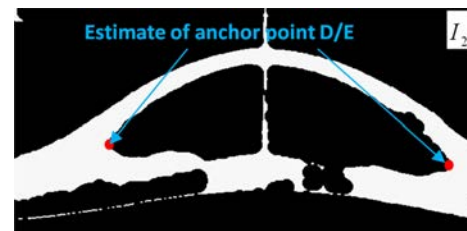
(a)
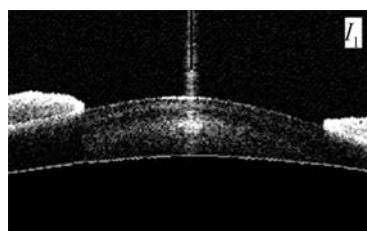
(b)

(c)

(d)

Fig. 3. (a) The anchor points A−E are marked as red points; the red, green, blue and magenta curves denote the endothelial surface of the central cornea, the endothelial surface of the peripheral cornea, the upper surface of the iris and the lens surface, respectively; (b) subimage I_1 where the anchor points B and C are located; (c) the curve C_1 generated from the pixel intensity accumulation of each column of I_1, where the points of discontinuity are marked as red points; (d) the binary image I_2 is obtained from the original AS-OCT image, where the estimate of anchor points D and E are marked as red points.

Area IV. We can extract their contours in different ways according to their particular characteristics.

3.3. *Extracting the inner contour*

A complete inner contour of the anterior chamber can be obtained by merging the endothelial surface of the cornea, lens surface and upper surface contours of the iris. The following focuses on how to extract each surface.

3.3.1. *The endothelial surface of the cornea*

For the cornea in Area III, the signal of the peripheral cornea is always very weak compared with

the signal of the central cornea and, therefore, a poor result is often obtained with the traditional edge detection algorithm,[9] as is shown in Fig. 4(b). To get a more accurate contour, we propose a method to fit the endothelial surface of the cornea with the points obtained by canny edge detector by three circular arcs under continuity constraints. In particular, the endothelial surface of the central cornea is fitted with one circular arc, as described in Sec. 3.1.1. The endothelial surface of the left peripheral cornea is fitted with one circular arc, which is restricted to pass the left end point of the endothelial surface of the central cornea that is the point of intersection between the endothelial surface of the central cornea and the perpendicular line
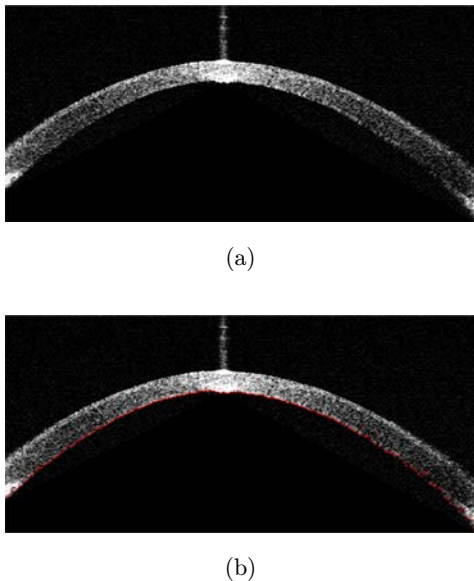
(a)

(b)

Fig. 4. (a) Cornea part extracted from the Area III in Fig. 3(a) (light beam crossings beneath the endothelial surface is removed by the divide-and-conquer strategy); (b) endothelial surface obtained by canny edge detector in the lower right is not desirable.

passing through the anchor point B. The endothelial surface of the right peripheral cornea can be obtained in a similar way. By using this new method, we can obtain an image of a continuous endothelial surface of the cornea, whose accuracy has been demonstrated by our experiments.

Fitting circular arcs under continuity constraints is a process that fits equations of circular arcs C_{circle} which pass a given point $P'(x', y')$ to the raw points $P_i(x_i, y_i)(1 \leq i \leq n)$. Suppose $O(x_0, y_0)$ stands for the center of C_{circle}, then the circle equation could be defined as $(x - x_0)^2 + (y - y_0)^2 = (x' - x_0)^2 + (y' - y_0)^2$. So the fitting error could be got:

$$f(x_0, y_0) = \sum_{1 \leq i \leq n} (2(x' - x_i)x_0 + 2(y' - y_i)y_0 + x_i^2 + y_i^2 - x'^2 - y'^2)^2. \tag{1}$$

Let

$$\begin{aligned} a_i &= 2(x' - x_i); \quad b_i = 2(y' - y_i); \\ c_i &= x_i^2 + y_i^2 - x'^2 - y'^2. \end{aligned} \tag{2}$$

Then, Eq. (1) becomes

$$f(x_0, y_0) = \sum_{1 \leq i \leq n} (a_i x_0 + b_i y_0 + c_i)^2. \tag{3}$$

In order to minimize $f(x_0, y_0)$, the following Eq. (4) should be satisfied:

$$\begin{cases} \dfrac{\partial f}{\partial x_0} = \sum_{1 \leq i \leq n} 2(a_i^2 x_0 + a_i b_i y_0 + a_i c_i) = 0, \\ \dfrac{\partial f}{\partial y_0} = \sum_{1 \leq i \leq n} 2(a_i b_i x_0 + b_i^2 y_0 + b_i c_i) = 0. \end{cases} \tag{4}$$

By solving Eq. (4), we can get

$$\begin{cases} x_0 = \dfrac{\sum_{1 \leq i \leq n} b_i c_i \sum_{1 \leq i \leq n} a_i b_i - \sum_{1 \leq i \leq n} a_i c_i \sum_{1 \leq i \leq n} b_i^2}{\sum_{1 \leq i \leq n} a_i^2 \sum_{1 \leq i \leq n} b_i^2 - \left(\sum_{1 \leq i \leq n} a_i b_i\right)^2}, \\ y_0 = \dfrac{\sum_{1 \leq i \leq n} a_i c_i \sum_{1 \leq i \leq n} a_i b_i - \sum_{1 \leq i \leq n} b_i c_i \sum_{1 \leq i \leq n} a_i^2}{\sum_{1 \leq i \leq n} a_i^2 \sum_{1 \leq i \leq n} b_i^2 - \left(\sum_{1 \leq i \leq n} a_i b_i\right)^2}. \end{cases} \tag{5}$$
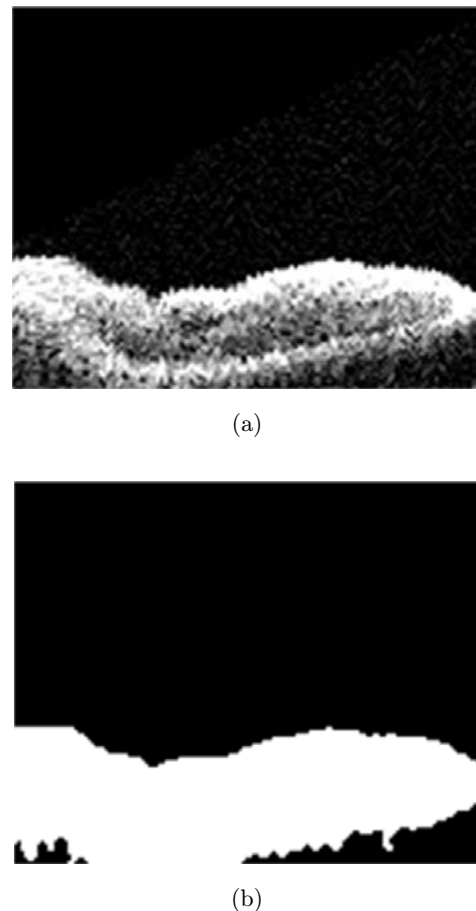

(a)

(b)

Fig. 5. (a) The left iris part extracted from Area I in Fig. 3(a); (b) the binary image obtained by filters and hole-filling method.

3.3.2. *The lens surface*

For the lens in the Area IV, canny edge detector is first used to get the primary upper contour, and then the contour is further fitted into a circular arc with RANSAC algorithm.

3.3.3. *The upper surface of the iris*

Taking the iris in Area I as an example, we show how to extract its upper contour. Filters such as the threshold filter, Gaussian filter and median filter are applied to it first, and the small connected regions are detected and filled. Because the signals of iris are usually very strong, we can obtain a binary image clearly, as is shown in Fig. 5(b). The upper surface of the iris could be extracted easily.

4. Experimental Results

An image set including more than 100 normal AS-OCT images is used to test the performance of our proposed method. All the images are of size 320×640 with 256 gray levels. The practical axial resolution of our AS-OCT imaging system is about $22\,\mu m$, and the transverse resolution is about $40\,\mu m$, while the system is completed with more than 9 mm imaging depth, which uses a broadband low-coherence light source with center wavelength of 1310 nm and a Fourier domain rapid scanning optical delay line (RSOD). An anterior segment OCT probe is designed, the scan mode is analyzed, and the obtained images are corrected by the AS-OCT system, where 400 A-Scans are obtained in 1 s.[10] The images were processed on an "Intel i5-2310 CPU" with 4096 MB of SDRAM. Our test showed that, for every image, the inner contour of the anterior chamber was extracted successfully within 0.2 s, as shown in Fig. 6, where upper contour of the central cornea is also displayed. By the way, the data processing speed would be increased with parallel algorithm.

An anterior segment analysis system with GUI has been developed to do the experiment, which was implemented in C++, as is shown in Fig. 7. Using this system, AS-OCT images could be analyzed automatically, the segment result and quantitative parameters could be viewed easily. Besides, A-Scans of the AS-OCT images could also be displayed by the system.
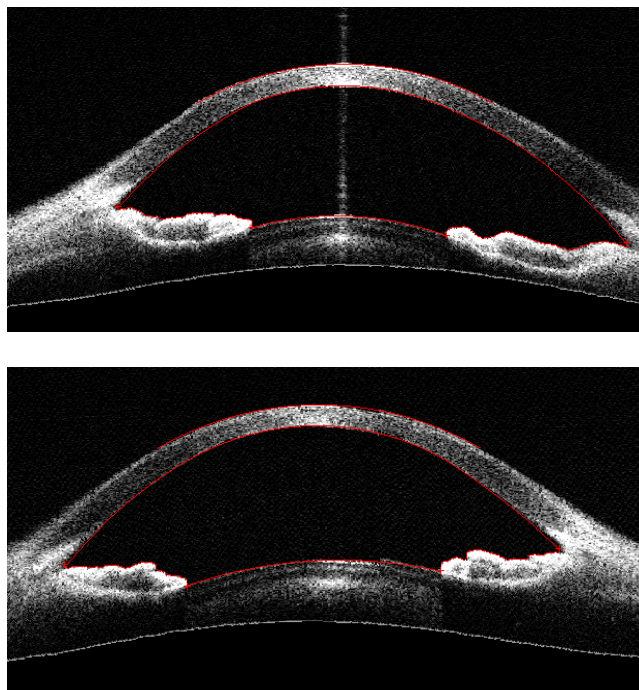

Fig. 6.   Two experimental results.

5. Discussion

Because of the characteristics of AS-OCT images, it is difficult to extract accurate inner contour by using global image segmentation methods directly, so the "divide-and-conquer" strategy is very important. Here, gray-scale morphology,[11] seed-grow segmentation[12] and watershed segmentation[13] are selected to do the experiments.

For the gray-scale morphology, the Gaussian filter and threshold filter are used first, and then the flat disk-shaped structuring element with the radius equaling 5 pixels is chosen as the kernel to do an open operation. For the seed-grow algorithm, the Gaussian filter and threshold filter are used to enhance the image first, then two points in the left/right anterior chamber are selected as the seeds to do region growing separately, then the results are merged together as the anterior chamber and the inner contour could be extracted easily. For the watershed algorithm, the Gaussian filter, median filter and threshold filter are used to obtain a binary image first, then the distance transform of the binary image is computed, and the black pixels are forced to be at negative infinity; finally the watershed transform is computed.

Experiments show that the three methods could not obtain a complete contour when the image is
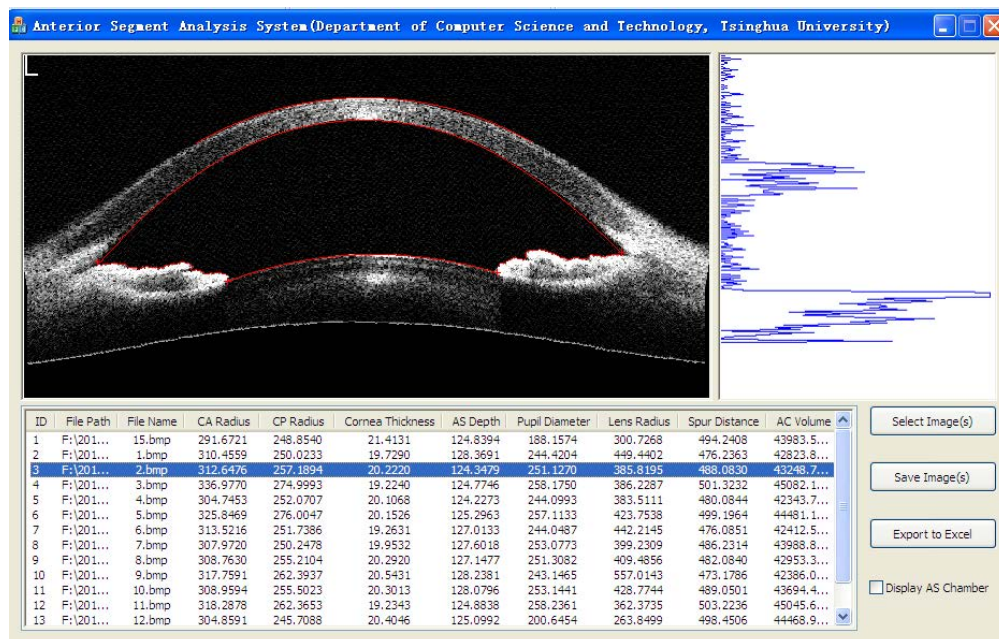
Fig. 7.   Our anterior segment analysis system with GUI, which is implemented by MFC. Using this system, AS-OCT images could be analyzed automatically, the segment result and quantitative parameters could be viewed easily. Besides, A-Scans of the AS-OCT images could also be displayed by the system.

(a)   (b)   (c)
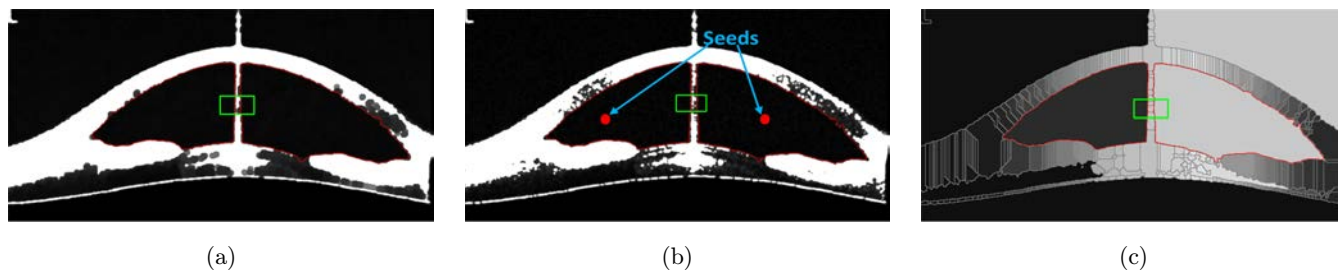
Fig. 8.   Experimental results of the classic global image segmentation algorithm after preprocessing methods are carefully selected and parameters optimization: (a) gray-scale morphology, the open operation[11]; (b) seed-grow segmentation,[12] the seeds are marked by red points; (c) watershed segmentation.[13]

affected by the light beam crossing, which are marked by green rectangles in Fig. 8. When the light beam crossing is removed manually, a complete contour could be extracted by the three methods, but the contour is not smooth enough in the peripheral cornea and lens part, sometimes even wrong when the edge signal is very weak, which are marked by green rectangles in Fig. 9. Besides, various filters are used many times to do preprocessing, which can help the classic methods to obtain a better result, but accordingly, some deviation of the inner contour of anterior chamber could not be avoided at the same time, especially in the anterior chamber angle area.

The classic global segmentation algorithms treat the image as a whole and the parameters or thresholds are the same for every part of the image, yet the AS-OCT image is composed of tissues with different characteristics, thus the classic global segmentation algorithms could not get a satisfying result, especially for the part where the edge signal is very weak. In contrast, our proposed method divides the image into subimages according to the detected anchor points and processes them with different strategies. In this way, the curve-fitting is easily used to obtain a smooth result when the edge signal is too weak.
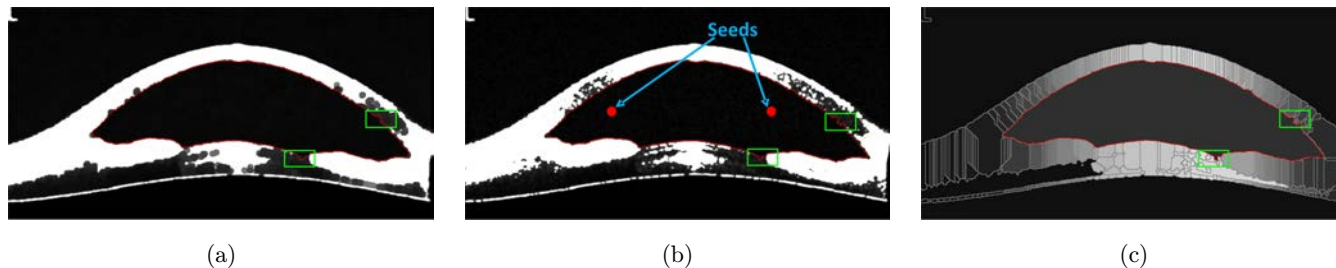
Fig. 9.   Experimental results of the classic global image segmentation algorithm after preprocessing methods carefully selected and parameters optimization, with the light beam crossing removed manually: (a) gray-scale morphology, the open operation[11]; (b) seed-grow segmentation,[12] the seeds are marked by red points; (c) watershed segmentation.[13]

It should be pointed out that the analysis of different regions for anterior chamber has been reported in Ref. 6. In Ref. 6, they assumed that the upper and lower boundary of the cornea shared the same circle center with the boundary of the lens, and it can be seen that the extracted contours there are rough. In our method, we abandon the aforementioned hypnosis in Ref. 6, and the endothelial surface of the cornea is fitted using three smoothing curves, such as circular arcs under continuity constraints. So a complete "divide-and-conquer" strategy is presented.

Our method deals with normal OCT images well, but it shows limitation for some abnormal images. In some cases, the anchor points may not be located correctly. For example, when the patient is affected by angle-closure glaucoma, the angle apex of the OCT images will be vague and difficult to identify, and our algorithm would find the wrong anchor points D/E, as is shown in Fig. 10. Manual calibration is necessary at this point. It should be noted that the identification of other anchor points and the calculation of central cornea thickness, pupil diameter, ACV and depth would not be affected. The improved method will be studied in the future: first the five anchor points are found automatically, then the result is checked by doctors and manual calibration is used if necessary, and the inner contour of anterior chamber is extracted according to the anchor points automatically in the end. On the other hand, in our method, the endothelial surface of the cornea is fitted using three circular arcs under continuity constraints, so it is very suitable for normal image analysis. For abnormal AS-OCT images, if endothelial surface of the cornea is changed greatly, the three smoothing curves fitting the endothelial surface of the cornea may be used. Others such as cubic B-spline, needs future investigations.
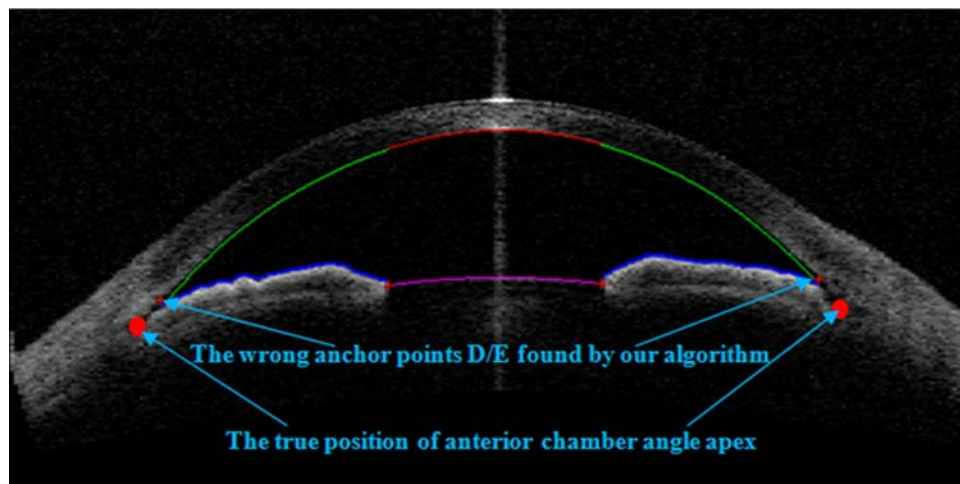

Fig. 10.   Experimental result of the OCT image affected by angle-closure glaucoma.

6. Conclusion

This paper reports a novel scheme for extracting the inner contour of the anterior chamber automatically from AS-OCT images. The proposed algorithm first detects the anchor points of an AS-OCT image and then divides it into subimages, where the endothelial surface of the cornea, the upper edge of the iris and lens upper surface are extracted using different schemes adapted to the particular characteristics of the subimages. In particular, it gives up the assumption that the upper and lower boundary of the cornea shared the same circle center, and proposes to fit the endothelial surface of the cornea using three smooth curves as circular arcs under continuity constraints. The experimental results show that the proposed algorithm can obtain the inner contour of the anterior chamber of an AS-OCT image accurately in real time.

Acknowledgments

References

1. M. Zysk, F. T. Nguyen, A. L. Oldenburg, D. L. Marks, S. A. Boppart, "Optical coherence tomography: A review of clinical development from bench to bedside," *J. Biomed. Opt.* **12**(5), 051403-1-21 (2007).

2. N. Wang, B. Wang, G. Zhai, K. Lei, L. Wang, N. Congdon, "A method of measuring anterior chamber volume using the anterior segment optical coherence tomographer and specialized software," *Amer. J. Ophthalmol.* **143**(5), 879−881 (2007).

3. S. Dorairaj, J. M. Liebmann, R. Ritch, "Quantitative evaluation of anterior segment parameters in the era of imaging," *Trans. Amer. Ophthalmol. Soc.* **105**, 99−110 (2007).

4. F. Graglia, J. L. Mari, J. Sequeira, Cornea contour extraction from OCT radial images (2010). Available at http://cdn.intechopen.com/pdfs/12357/InTech-cornea_contour_extraction_from_oct_radial_images.pdf (accessed May 1, 2012).

5. A. Coron, R. H. Silverman, A. Saied, P. Laugier, "Automatic segmentation of the anterior chamber in *in vivo* high-frequency ultrasound images of the eye," in *Proc. Ultrasonics Symposium, IEEE*, pp. 1266−1269, New York (2007).

6. L. F. Lin, Y. Ju, "Automatic extraction of the anterior chamber contour in OCT images," in *Proc. Second Int. Symp. Inform. Sci. Engrg.* pp. 423−426, Shanghai (2009).

7. C. K. Leung, H. T. Li, R. N. Weinreb, J. Liu, C. Y. Cheung, R. Y. Lai, C. P. Pang, D. S. Lam, "Anterior chamber angle measurement with anterior segment optical coherence tomography (OCT) — A comparison between slit lamp OCT and visante OCT," *Invest. Ophthalmol. Vis. Sci.* **49**(8), 3469−3474 (2008).

8. M. A. Fischler, R. C. Bolles, "Random sample consensus: A paradigm for model fitting with applications to image analysis and automated cartography," *Commun. ACM* **24**(6), 381−395 (1981).

9. J. Canny, "A computational approach to edge detection," *IEEE Trans. Pattern Anal. Mach. Intell.* **8**(6), 679−698 (1986).

10. S. D. Cai, Y. H. He, H. Li, Z. F. Li, P. Li, X. S. Dai, L. Wu, "Study of the eye anterior segment imaging system with optical coherence tomography," *J. Optoelectron. Laser* **21**(4), 628−631 (2010).

11. H. M. Robert, S. R. Robert, X. H. Zhuang, "Image analysis using mathematical morphology," *IEEE Trans. Pattern Anal. Mach. Intell.* **9**(4), 532−550 (1987).

12. R. C. Gonzalez, R. E. Woods, *Digital Image Processing*, 2nd Edition, Prentice Hall, New Jersey (2002).

13. L. Vincent, P. Soille, "Watersheds in digital spaces: An efficient algorithm based on immersion simulations," *IEEE Trans. Pattern Anal. Mach. Intell.* **8**(6), 583−598 (1991).